ESD-TR-67-41

Technical Note

1967-7

Monte Carlo Simulation of the Flow of a Rarefied Gas Around a Cylinder

A. W. Starr

18 January 1967

Prepared for the Advanced Research Projects Agency
under Electronic Systems Division Contract AF 19(628)-5167 by

Lincoln Laboratory
MASSACHUSETTS INSTITUTE OF TECHNOLOGY
Lexington, Massachusetts

The work reported in this document was performed at Lincoln Laboratory, a center for research operated by Massachusetts Institute of Technology. This research is a part of Project DEFENDER, which is sponsored by the U.S. Advanced Research Projects Agency of the Department of Defense; it is supported by ARPA under Air Force Contract AF 19(628)-5167 (ARPA Order 600).

Distribution of this document is unlimited.

MASSACHUSETTS INSTITUTE OF TECHNOLOGY

LINCOLN LABORATORY

MONTE CARLO SIMULATION OF THE FLOW OF A RAREFIED GAS AROUND A CYLINDER

A. W. STARR

Group 35

TECHNICAL NOTE 1967-7

18 JANUARY 1967

LEXINGTON MASSACHUSETTS

ABSTRACT

A Monte Carlo technique is described for simulating the high-speed flow of a rarefied gas around a cylindrical body. The method uses a hard-sphere model, or, alternatively, the "Maxwellian" model to compute collisions between particles. A representative "test particle" is scattered in such a way that its statistical behavior approximates that of a random particle chosen from the actual gas. This requires knowledge of the distribution function of "target" particles, which is estimated from observations of the behavior of the test particle.

The method is applicable to any collision model and to any model for the interaction between the gas and the surface of the body.

Accepted for the Air Force
Franklin C. Hudson
Chief, Lincoln Laboratory Office

TABLE OF CONTENTS

I. INTRODUCTION

Many attempts have been made to solve analytically the problem of high speed flow of a rarefied gas around various simple aerodynamic bodies. Although some progress has been made, exact solutions are not yet available even for very simplified boundary conditions and gas models. When the physics of the problem is described more realistically, it becomes very difficult to get even approximate solutions which agree with experimental observations.

One technique which may be used to circumvent the analytical difficulties is the "direct" Monte Carlo simulation. In such an approach, the gas is modeled by a collection of "particles", generally much fewer in number than the number of particles in the actual gas. These particles are made to behave as actual gas particles would, that is, they are affected by the same statistical laws that govern the actual distribution of particle velocities and positions. By observing these "test" particles for a sufficiently long time, one can then deduce their distribution function, which when properly normalized should be the distribution function for particles in the actual gas. Since all aerodynamic properties can be deduced from the distribution function, it constitutes a complete solution to the problem.

An "incident" particle can be made to behave statistically as if it were a typical member of the actual gas only if one

knows:

(1) the mechanism governing collisions between particles,

(2) the interaction between gas particles and any solid surface which they may strike,

(3) the density and velocity distribution of the "target" particles which scatter the incident particle.

The first requirement is easily met by postulating a collision model, either based upon empirical data or upon some repulsive force law chosen for analytic simplicity. Similarly, a model for the particle-surface interaction may be chosen. The third requirement, however, requires knowledge of the distribution function, which is the object of the calculation. Thus, the simulation envisioned here must be iterative in nature, hopefully converging to the correct answer after a sufficiently long run under constant conditions. The test particles must be scattered by a collection of particles distributed in velocity space according to the latest estimate of the true distribution. In turn, it must be possible to improve this estimate by incorporating information gained by observing the behavior of the scattered particles.

II. REVIEW OF PREVIOUS MONTE CARLO GAS SIMULATIONS

Only a few attempts have been made at solving problems in gas dynamics by direct simulation. One of the earliest was by Alder and Wainwright[1], who followed the exact motion of about 100 rigid elastic particles. Bird[2] solved by a Monte Carlo method for the relaxation to thermal equilibrium of about 1000 hard sphere particles, starting with all the particles moving at the same speed but in random directions. A similar calculation, using two different collision models, has recently been performed here.[3]

The calculations described above were essentially zero-dimensional (in position space), since all the particles were in effect located at a single point.

Lavin and Haviland[4,5,6] treated two more significant problems by the Monte Carlo method: heat transfer between two parallel planes, and the one-dimensional shock wave. Both problems are one-dimensional in position space, and symmetry allowed the problem to be posed in a three-dimensional phase space consisting of the position along the line normal to the planes, the velocity along this same line, and the magnitude of the velocity component parallel to the planes. With only three dimensions, it was feasible to divide all of phase space into cells of appropriate size. In each cell was stored a single scalar number giving the value of the distribution function. A single test particle was introduced at one surface

with a random thermal velocity corresponding to the temperature at that surface. It was then advanced ballistically from cell to cell in phase space. If it struck a surface, it was re-emitted randomly at the temperature of the surface. When necessary, collisions were computed. This could easily be done, since an approximation to the distribution function was always available. By observing the single test particle for a long time, the current approximation to the distribution function could then be improved. This method attempts an exact solution to the problem (i.e., the distribution at all points in space) and is limited by the coarseness of the grid of cells and by the computing time required for statistical fluctuations to average out. It is also evident that if the Knudsen number (the ratio of mean free path to some characteristic length) were too small, an excessive number of collisions would have to be computed. Finally, one would prefer an initial distribution which is somewhere near the expected true distribution. Otherwise, it is not clear that the test particle would be scattered in such a way as to yield an improved estimate.

While the method of Haviland and Lavin produces good results for one-dimensional problems, it is not easily extended to problems lacking the symmetry needed to reduce phase space to three dimensions. To divide a five- or six-dimensional phase space into a grid of cells, even if the grid is very coarse, would exceed the storage capacity of most computers. Furthermore,

the distribution function (which is proportional to the fraction of the time a given particle spends in a particular cell in phase space) is estimated by averaging the behavior of the test particle for a very long time. Thus the test particle must enter each cell a large number of times before meaningful averages can be obtained. Thus not only the storage requirements but also the computation time increases by many orders of magnitude in going from three- to five- or six-dimensional phase space.

Fortunately, in most gas dynamics problems, only certain averages of the distribution function over all velocity space are required, e.g., density, temperature, mean velocity, etc., rather than the velocity distribution itself. Such averages can be obtained quite accurately even from a rather crude approximation to the distribution function, provided that the approximation is not biased. Thus a Monte Carlo method may provide useful information even when there is not enough symmetry to reduce phase space to three dimensions.

Probably the greatest success in this direction has been achieved by Bird [7], who applied a novel method to problems with either axial or cylindrical symmetry. In these problems (which include gas flow around cylinders, spheres, flat plates, cones, etc.) phase space is reduced to five dimensions by ignoring one position coordinate. Bird stores the two positions and three velocity components of a small number of particles (about 1000)

to represent his model gas, and does not divide phase space into cells. In order to determine whether or not a given "incident" particle collides at a particular location, one must have some representation of the distribution function of "target" particles at that point. Bird uses as this representation the particles which, at the given instant, happen to lie within a sphere centered at the would-be collision site. This sphere is large enough to give a reasonably large choice of collision partners. A large number of such collisions are calculated (the details of this process are described in Bird's paper) using the "hard sphere" collision model with the entire collection of particles frozen in position. Then all the particles are advanced ballistically (without collisions) for a time equal to the accumulated mean waiting times for each of the collisions which were calculated. The procedure is done in such a way that each particle has the prescribed mean free path. Samplings are made at intervals long enough to permit decorrelation, and the desired aerodynamic quantities are obtained from ensemble averages of many samples. Bird presents density profiles, drag coefficients, and various other aerodynamic quantities of interest for various Knudsen numbers, stream speeds, body temperatures, and body geometries.

While Bird's method produces impressive results, the process by which convergence occurs is a subtle one whose validity is not easy to eastablish. Thus it seems desirable to find some

alternative Monte Carlo technique whose results could be compared with Bird's. Such a method will be described in detail below.

III. BRIEF DESCRIPTION OF THE PRESENT CALCULATION

The model used in this calculation may be regarded as a compromise between the technique of Haviland and Lavin and Bird's method. Haviland and Lavin divided all of phase space into cells. Bird used no cells but rather a single list of particles to represent his distribution function. For this calculation, position space is divided into a two-dimensional grid of cells, while the velocity distribution in each cell is represented by a list of four-vectors. The first three components are the velocity components of a "target particle", while the fourth component is a weighting factor.

In a given cell, the true continuous velocity distribution is thus replaced by a collection of delta functions whose locations are given by the first three components and whose areas are given by the fourth component. When calculations of collision rates and selection of collision partners call for a velocity distribution, this collection of "spikes" is normalized by dividing by the sum of all the fourth components. It may then be treated mathematically as if it were the true continuous velocity distribution. The"particles" on this list (a different list for each cell) have no purpose other than to serve as a local representation of the velocity distribution. They are <u>not</u> moved ballistically from cell to cell, as are Bird's particles.

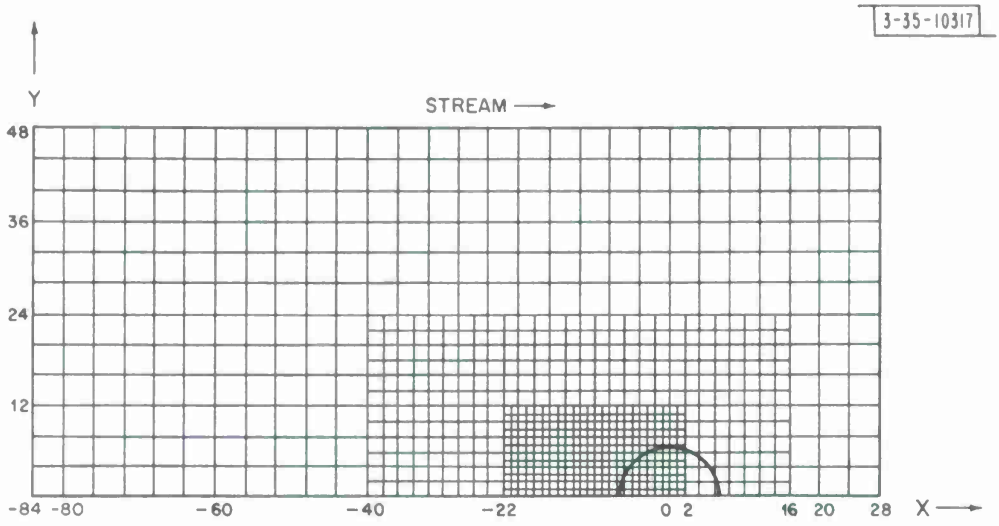

Figure 1. The grid of cells in position space. The radius of the cylinder is $\sqrt{45}$. The lower left corners of some typical cells are listed below, in order to illustrate the numbering system.

Cell (1, 1)	at	(-22, 0)
Cell (1, 12)	at	(-22, 11)
Cell (24, 12)	at	(1, 11)
Cell (25, 1)	at	(-40, 0)
Cell (33, 12)	at	(-24, 22)
Cell (34, 6)	at	(-22, 22)
Cell (34, 12)	at	(-24, 22)
Cell (40, 1)	at	(2, 0)
Cell (46, 12)	at	(14, 22)
Cell (47, 1)	at	(-84, 0)
Cell (57, 12)	at	(-44, 44)
Cell (58, 6)	at	(-40, 44)
Cell (58, 12)	at	(-36, 44)
Cell (64, 7)	at	(12, 24)
Cell (65, 1)	at	(16, 0)
Cell (67, 12)	at	(24, 44)

There are a total of 804 cells.

The formation of the lists and their statistical justification will be described later. The actual grid of cells used is shown in Figure 1. Because finer structure and higher density are expected near the cylinder than far away from it, three different cell sizes are used in the grid. The stream velocity is in the x-direction* and the axis of the cylinder is in the z-direction. The entire grid is bounded by the plane of symmetry ($y = 0$) and by upstream, downstream, and side boundaries far from the cylinder. It is assumed that collisions outside these boundaries will not appreciably affect conditions near the cylinder.

Like the calculation of Haviland and Lavin, this method used only one "test particle" which wanders from cell to cell. The process begins by generating a test particle at a random position along an end or side boundary with the free upstream velocity plus a randomly generated thermal velocity.

The test particle then enters the first cell, and the time required to traverse the cell is computed. The collision rate (which depends on the collision model, the test particle velocity, the local density and the local velocity distribution) is calculated, and a random "time-to-collision" is then drawn from

---

*A component of stream velocity in the z-direction could also be added without destroying symmetry, but this has not been done in the first calculations.

the appropriate distribution. If this time is greater than the time to traverse the cell, no collision occurs and the test particle is advanced to the beginning of the next cell. (The traversal of the cell by the test particle clearly provides information about the distribution function; this information is incorporated into the current estimate for the cell by a process to be described later.) If the time to collision is less than the time to the cell wall, a collision will occur. The test particle is then first advanced ballistically to the site of the collision, and the information gained from this portion of the trajectory is incorporated into the current estimate for the cell. Then a velocity for the "collision partner" is drawn randomly from the list (the actual drawing depends on the collision model) and a pair of collision parameters (again dependent on the collision model) is drawn. The new velocity of the test particle is then calculated. The list of velocities representing the distribution function is not directly affected by the collision.

Using the new velocity, the time to the wall and the time to the next collision are recalculated, and the process continues. There is no inherent limitation on the number of collisions which may occur during one passage through a cell, but multiple collisions during one passage will be rare due to the long mean free path. The number of updatings (the incorporation of information from a straight segment of the test particle trajectory)

corresponding to a single passage through a cell is one greater than the number of collisions occurring during that passage.

Thus the test particle wanders from cell to cell, occasionally undergoing a collision which changes its velocity. Whether or not it collides in a particular cell, the fact that it passed through contains information about the local density and velocity distribution. This information must be added to the current local estimate to produce an improved estimate. One way to do this would be simply to add one more velocity to the list, namely the test particle velocity. The weighting factor would be the time the particle spent in the cell during its passage. This is necessary in order that particles which remain in the cell a long time contribute more to the density than those particles which go through very quickly. This also takes proper account of trajectories which barely cut across the corner of the cell.

This procedure would eventually produce lists which would be too long for the storage capacity of the computer. Even if this were no problem, the distribution function represented by a very long list would not be appreciably changed by the addition of one more four-vector, so convergence would be very slow. Thus, the actual procedure followed is to let the list grow to a maximum length (not more than 22 in this version). After the maximum length has been reached, an entry is deleted every time a new entry is added. Thus an entry remains on the list for

n passages of the test particle, where n is the length of the list.*

While the deletion of entries from the list destroys some of the information, the features of the distribution function of greatest interest, e.g., density, mean velocity, temperature and certain other higher moments of the distribution, are accumulated in positions on the list reserved for this purpose. Thus the current estimates of mean velocity and density are not based merely upon the small collection of four-vectors currently on the list, but upon all entries which have been on the list since the last time the velocity and density accumulators were reset to zero.

When the test particle strikes the body, it is absorbed and re-emitted at the same point according to the model chosen to represent the surface. A procedure often used for analytic work, and also used here, is to re-emit a fraction α diffusely, and the rest specularly. Diffuse emission is equivalent to having a small hole in the surface at the absorption point, behind which is a gas in equilibrium at some temperature T_b. When a particle is absorbed, a shutter in front of the hole is opened and a single particle is allowed to pass outward. This sort of emission follows the usual cosine law, and the velocity

---

*An alternative representation of the velocity distribution is described in the appendix.

of the emitted particle is uncorrelated with that of the absorbed particle. Specular reflection simply reverses the normal component of velocity. The fraction α which is emitted diffusely is called the accommodation coefficient.

This surface model, with α near unity, is considered reasonable for the low densities of interest in this problem. However, it would not be difficult to use a more complicated model based on experimental observations.

When the test particle strikes the plane of symmetry, it is reflected specularly. When it crosses a side or end boundary, it is lost. A new test particle is then generated with position and velocity uncorrelated with those of the old test particle. A certain fraction of the particles must be generated along the side boundary in order to compensate for downstream depletion through the sides (which would occur even if the body were absent). This fraction depends upon the ratio of the stream speed to the thermal speed and is calculated at the beginning of the computation.

The velocity of the newly generated test particle is then formed by adding a random thermal velocity to the x-directed stream velocity. If a particle is to be generated at an end boundary (a result of drawing a rectangular random number greater than the fraction to be introduced at the side), it is given a random y-coordinate along the upstream or downstream boundary,

depending on the sign of the x-component of velocity. If it is introduced at the side boundary, its y-velocity is always negative.

After a predetermined number of particles have been lost through the end and side boundaries, a sample is taken. Only the "cumulative registers" in the individual cells contribute to the sampling. From these cumulative registers are formed arrays showing the density (normalized to free-stream density), the mean velocity, the thermal velocity spread and the energy flow vector (normalized to free-stream energy flow) corresponding to the center of each cell. The net momentum and energy transfer to the body is also stored, and from this the drag coefficient and other aerodynamic quantities can be calculated. The contents of various other counters showing the progress of the calculation are also printed, e.g., number of collisions, average free path between collisions, etc.

After the sampling has been completed, one could simply resume the calculation. However, if this is done, observations on the test particle taken long ago will be weighted equally with the latest observations, even though the latest are presumably based on an improved estimate of the distribution function of the scatterers. On the other hand, the cumulative registers may not be reset to zero, since then all information based on earlier calculation would be lost. The procedure

adopted here is to decide (perhaps somewhat arbitrarily) the relative weights to be attached to prior and new data. The cumulative registers in every cell (but not the numbers of the list representing individual particles) are multiplied by some number less than unity, such that they will appear to have been generated by a smaller number of particles than actually was used. The details of this "downgrading of prior information" will be explained later.

Generally, it is desired to perform the calculation for a series of Knudsen numbers at a fixed stream speed. The calculations are performed in decreasing order of Knudsen number, always starting with the free molecular case (infinite Knudsen number). At the start, all cells are empty, and there is thus no estimate of the distribution function available, and no collisions can be calculated. This poses no difficulty for free molecular flow, since the particles do not interact and the collision calculations can be bypassed. When the free molecular solution has been found, it serves as a first approximation to the solution for the highest finite Knudsen number, etc. As the Knudsen number is lowered, the convergence will become slower, since more collisions will be calculated, and eventually limitations on computer time will force a halt to the computation.

The program is written to compute collisions by either the hard-sphere or the "Maxwellian" (inverse fifth power repulsion)

molecular model. A subroutine could also be written to compute collisions by some empirical model, if the two simple models are considered too unrealistic.

Provision is made for writing all variable values on a tape, so that the computation could be continued at a later time after examination of the data.

The mathematical basis of the calculation is presented in Section IV. When results are available, they will be presented in a subsequent report.

IV. MATHEMATICAL BASIS OF THE SIMULATION

In this section the mathematical basis of the various parts of the simulation will be presented. Much of the same material is presented somewhat more generally elsewhere, especially by Patterson[8], Haviland[5], and Lavin[4]. The treatment here is intended as a derivation and explanation of the method used in the program and thus follows it closely in order and in nomenclature.

(1) Dynamics of elastic collisions

Consider two particles of equal mass and velocities $\vec{v}_1$ and $\vec{v}_2$ which collide elastically. Their velocities after collision are $\vec{v}_1'$ and $\vec{v}_2'$. Their relative velocity before collision is

$$\vec{v}_r = \vec{v}_1 - \vec{v}_2. \tag{1}$$

From conservation of momentum,

$$\vec{v}_1 + \vec{v}_2 = \vec{v}_1' + \vec{v}_2', \tag{2}$$

and from conservation of energy,

$$v_1^2 + v_2^2 = v_1'^2 + v_2'^2, \tag{3}$$

where $v_1 = |\vec{v}_1|$, etc. Combining equations (2) and (3), we obtain

$$v_r' = v_r$$

$$\vec{v}_1' = 1/2(\vec{v}_1 + \vec{v}_2) + 1/2\ \vec{v}_r' \tag{4}$$

$$\vec{v}_2' = 1/2(\vec{v}_1 + \vec{v}_2) - 1/2\ \vec{v}_r'.$$

Note that equations (4) are seven scalar equations in nine unknowns. The remaining two unknowns correspond to the direction of the new relative velocity. This depends on the particular collision model, on the collision parameters and on $\vec{v}_r$.

(2) Collision mechanics for a general repulsive force law

Assume a repulsive force K/r^n per unit mass between the two molecules, where $\vec{r} = \vec{x}_1 - \vec{x}_2$. Then the equation of motion is easily shown to be

$$\ddot{\vec{r}} = 2K\vec{r}/r^{n+1}. \tag{5}$$

In polar coordinates these equations may be written (see Figure 2)

$$1/2(\dot{r}^2 + r^2\dot{\theta}^2) + \frac{2K}{n-1}\, r^{1-n} = \text{const} = 1/2\ v_r^2 \tag{6}$$

$$r^2\dot{\theta} = \text{const} = bv_r,$$

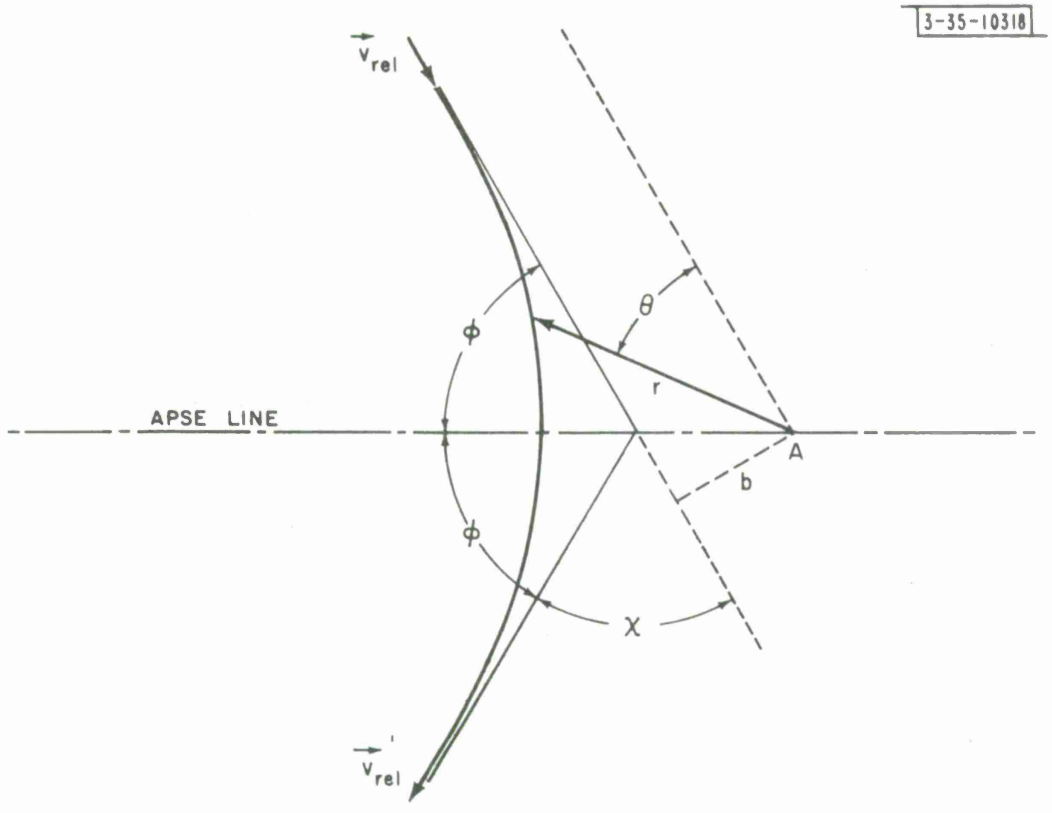

Figure 2. The coordinate system in the collision plane for a repulsive force law.

where b is the distance by which they would miss each other if no interaction occurred.

Eliminating time from (6),

$$\frac{dr}{d\theta} = -\sqrt{\frac{r^4}{b^2} - r^2 - \frac{4Kr^{5-n}}{(n-1)b^2 v_r^2}} \quad . \tag{7}$$

Introducing the dimensionless coordinate

$$W = b/r, \tag{8}$$

and letting $W_o = b\left(\frac{v_r^2}{2K}\right)^{1/n-1}$, (9)

equation (7) takes the form

$$\frac{dW}{d\theta} = \sqrt{1 - W^2 - \frac{2}{n-1}\left(\frac{W}{W_o}\right)^{n-1}} \tag{10}$$

Now at the point of closest approach

$$\frac{dW}{d\theta} = \frac{dW}{dr}\ \frac{dr}{d\theta} = 0.$$

This is the intersection with the apse line, and corresponds to the angle ϕ in Figure 2 and to $W = W_o$. Thus we can integrate (10) to get

$$\phi = \int_0^{W_1} \left[1 - W^2 - \frac{2}{n-1} \left(\frac{W}{W_o}\right)^{n-1}\right]^{-1/2} dW = \phi(W_o), \qquad (11)$$

where $W_1(W_o)$ is a positive root of

$$1 - W^2 - \frac{2}{n-1} \left(\frac{W}{W_o}\right)^{n-1} = 0. \qquad (12)$$

The collision angle (the angle between the new and old relative velocities) is then

$$\chi(W_o) = \pi - 2\phi(W_o). \qquad (13)$$

(3) Maxwellian molecule

When n = 5, the above equations assume a simple form. A molecule with this force law is called a "Maxwellian" molecule. Note that W_o is a function of the magnitude of the relative velocity and of the collision parameter b (the "miss distance").

Setting n = 5, equation (11) can be integrated. The collision angle then is

$$\chi(W_o) = \pi - \frac{2}{(1+2/W_o^4)^{1/4}} K\left[1/2 - 1/2\left(1 + \frac{2}{W_o^4}\right)^{-1/2}\right], \qquad (14)$$

where $K(\alpha)$ is the complete elliptic integral of the first kind:

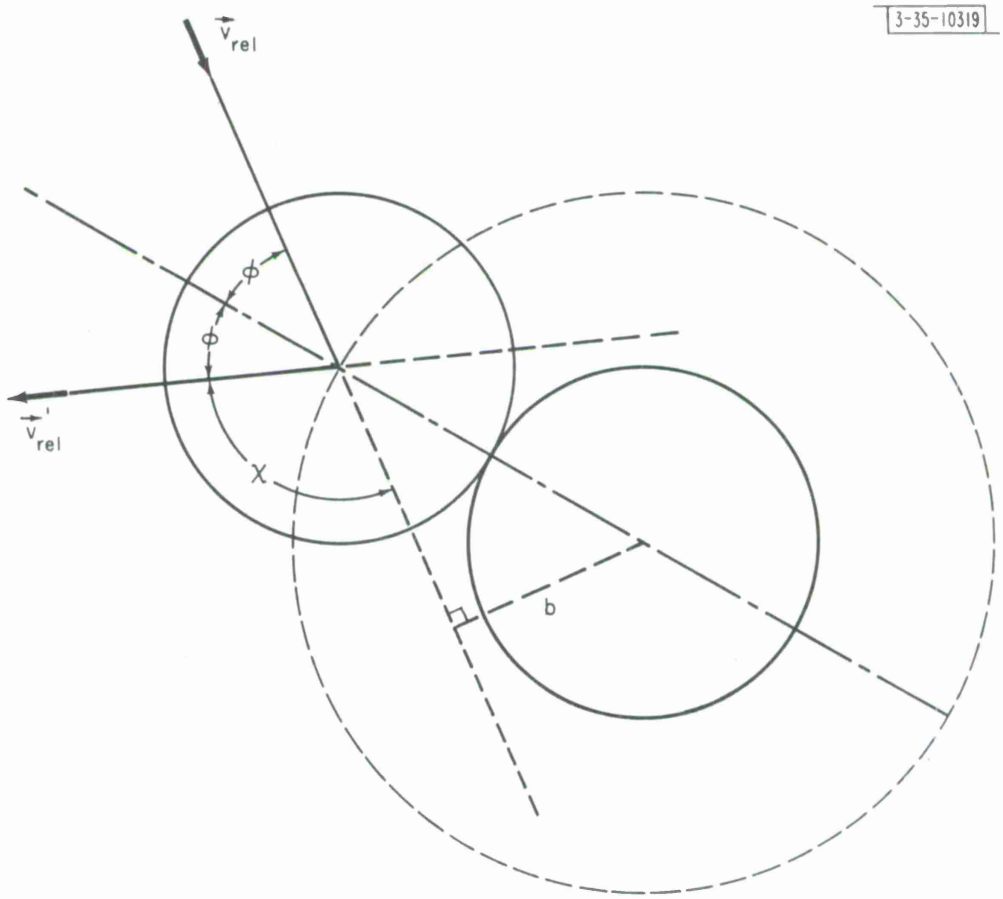

Figure 3. Collision geometry for hard sphere molecules.

$$K(\alpha) = \int_0^{\pi/2} \frac{dy}{\sqrt{1 - \alpha \sin^2 y}} \qquad (15)$$

(4) Hard sphere molecule

The "hard sphere" molecule is a limiting case of the inverse power molecule. The scattering angle χ then becomes independent of the speeds of the particles, depending only on the "miss distance" b. It is easily seen from the diagram of the collision in Figure 3 that

$$b = R \cos(\chi/2) \qquad (16)$$

(5) Calculation of velocities after collision

For both Maxwellian and hard sphere molecules, it has been shown above how to calculate χ, the angle between the new and old relative velocities, given the magnitude of the relative velocity v_r and the "miss distance" b (only the latter is required for the hard sphere molecule). In addition to the scattering angle χ, there is another angle, ϵ, which must be known before the collision is completely specified. It is the angle between the plane containing the new and old relative velocities and some arbitrary plane containing the old relative velocity. The range of χ is from 0 to π, while ϵ varies from 0 to 2π. The calculation of ϵ is very simple for any central force law. With any

isotropic scattering model, all values of ϵ from 0 to 2π are equally likely.

Once ϵ and χ are known, the new velocities can be computed as follows:

Form a set of three unit vectors $\vec{z}_1$, $\vec{z}_2$, and $\vec{z}_3$ such that $\vec{z}_1$ is parallel to the old relative velocity. The new relative velocity is then

$$v_r' = v_r(\vec{z}_1 \cos\chi + \vec{z}_2 \sin\chi \cos\epsilon + \vec{z}_3 \sin\chi \sin\epsilon) \qquad (17)$$

The unit vectors $\vec{z}_1$, $\vec{z}_2$, and $\vec{z}_3$ may themselves be expressed in terms of $\vec{z}_x$, $\vec{z}_y$, and $\vec{z}_z$, and equation (4) may then be used to compute the new velocities $\vec{v}_1'$ and $\vec{v}_2'$. This applies to any scattering model.

An even easier procedure is available for the hard sphere molecule, based on the peculiar fact that in a hard sphere collision the direction of $\vec{v}_r'$ is independent of the direction of $\vec{v}_r$, and hence may be chosen randomly.

(6) Selection of collision parameters

Suppose b_{max} is the maximum miss distance for which collisions are to be calculated. Then, in the plane containing the target particle and normal to the trajectory of the incident particle, let a circle of radius $2b_{max}$ centered at the target

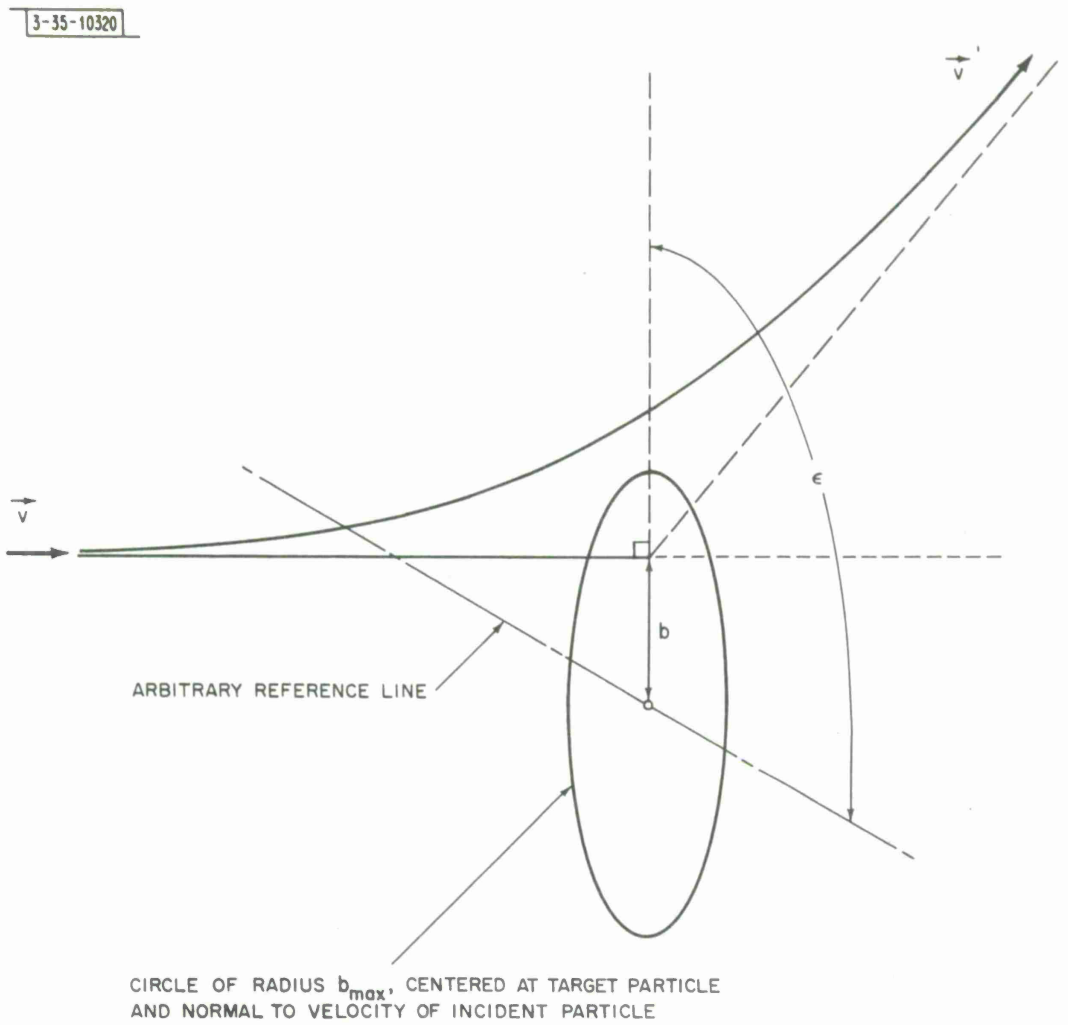

Figure 4. Geometry of collision parameters for binary collisions. Orbit lies in plane containing target particle.

particle be drawn (Figure 4). If it has been decided that the two particles shall collide, then the trajectory of the incident particle (in the coordinate system of the target particle) must intersect this infinitesimal circle. Clearly there can be no variation in the distribution function over such a small circle, so all intersection points are equally likely. If R_1 and R_2 are two rectangular* random numbers, a random point inside the circle is given by

$$\epsilon = 2\pi R_1,$$
$$b^2 = b_{max}^2 R_2. \tag{18}$$

This is the procedure for choosing collision parameters.

(7) Calculation of collision rates

In the Monte Carlo scheme, a test molecule enters a cell, and we must decide

(1) whether or not a collision will occur, and

(2) in the event of a collision, the velocity of the collision partner.

To make these decisions we must know the scattering model, the

*"Rectangular" random numbers are uniformly distributed between 0 and 1.

velocity of the test molecule, and the density and velocity distribution of "target" molecules in the cell.

Now consider two beams of particles of velocities $\vec{v}_1$ and $\vec{v}_2$ which intersect such that their collision parameters are within the element area b db dϵ, in the coordinate system of the target beam. Then in a time interval dt, all the particles in the incident beam lying within the volume element v_r b db dt dϵ will collide. Summing over both collision parameters gives us the collision integral:

$$X(\vec{v}_1, \vec{v}_2) = \int_o^{2\pi} d\epsilon \int_o^{b_{max}} v_r \, b \, db \qquad (19)$$

This is the volume per unit time of the incident beam which collides with the target beam.

For the hard sphere, b_{max} is obviously twice the radius of the sphere. For other collision models, the choice is not obvious, since collisions can occur for any value of b. Normally we do not wish to waste time computing grazing collisions, so we choose b_{max} such that collisions with deflection angle χ less than some minimum value (usually about 11^o) will be ignored. This generally makes b_{max} a function of velocity. For the Maxwellian molecule, equation (14) shows that it is W_o which has a fixed maximum value (independent of velocity) for a fixed minimum scatter angle. Thus instead of choosing $b = b_{max} R_1$, as

in (18), it is more convenient to choose $W_o = W_{o\ max}\ R_1$.

The collision rate $\sigma(\vec{v}_1)$ is then obtained by integrating over the distribution $f(\vec{v}_2)$ of target particles:

$$\sigma(\vec{v}_1) = \int_{all\ \vec{v}_2} d\vec{v}_2\ f(\vec{v}_2)X(\vec{v}_1,\ \vec{v}_2). \tag{20}$$

For hard sphere molecules, the collision rate is easily found from equations (19) and (20):

$$\sigma(\vec{v}_1) = \pi r^2 \int_{all\ \vec{v}_1} v_r f(\vec{v}_2,\vec{x})\ d\vec{v}_2, \tag{21}$$

where r is the radius of the hard sphere.

For the Maxwellian molecule, we use equations (9) (with n = 5) and equations (19) and 20) to obtain

$$\sigma(\vec{v}_2) = \rho\pi W_{o\ max}^{\ 2}\ (2K)^{1/2}, \tag{22}$$

where $\rho(\vec{x}) = \int_{all\ v_1} f(\vec{v}_2,\vec{x})d\vec{v}_2$ is the local number density.

It was shown by Haviland[5] that a value of $W_{o\ max}$ of about 1.5 gave good results (this corresponded to a cut-off of about 11^o for the scatter angle).

(8) Mean free path

In the Monte Carlo simulation, the stream speed and the Knudsen number are specified, and parameters such as K in equation (22) and r in equation (21) are not meaningful. To eliminate these parameters from our equations, we consider the mean free path λ.

Patterson[8] shows that the mean free path for hard spheres of radius r is

$$\lambda = \frac{1}{\sqrt{2}\pi r^2 \rho} \tag{23}$$

while for Maxwellian molecules,

$$\lambda = \frac{2}{\pi^{3/2} \rho W_{o\ max}^2} \left(\frac{kT}{K}\right)^{1/2}. \tag{24}$$

Now, since $W_{o\ max}$ is arbitrary, this gives an arbitrary mean free path. Haviland[5] shows that the "effective mean free path" (based on comparisons of viscosity and heat conduction with other collision models) is

$$\lambda_{eff} = \frac{1}{2\pi(0.436)\rho} \left(\frac{kT}{K}\right)^{1/2}. \tag{25}$$

Thus, if we want to specify a certain mean free path (for comparison with other models) λ_{eff}, we choose

$$\left(\frac{kT}{K}\right)^{1/2} = 2\pi(0.436)\rho\lambda_{eff}. \tag{26}$$

The mean free path in the computation process then is (for the Maxwellian molecule)

$$\lambda = \frac{4(0.436)\lambda_{eff}}{\pi W_{o\ max}^2} \tag{27}$$

(9) Representation of the distribution function of a finite collection of particles

In the present Monte Carlo scheme the velocity distribution is represented by a set of N "particles" with velocities $\vec{v}_i$ and associated weighting factors w_i. At a given instant, this is a crude representation, but in the long run an ensemble average of these collections should give a good approximation to the true distribution function.

Assuming a collection of particles has been "correctly" selected, we focus our attention on computation of the collision rate, and when necessary, the selection of a collision partner.

At any instant, our estimate of the distribution function is a finite collection of "spikes":

$$f_{est}(\vec{v}) = \frac{\rho_{est} \sum_{i=1}^{N} w_i\ \delta(\vec{v} - \vec{v}_i)}{\sum_{i=1}^{N} w_i} \tag{28}$$

where $\delta(\vec{v})$ is the usual Dirac delta function, i.e.,

$$\iiint_{\text{all } \vec{v}} dv_x dv_y dv_z \delta(\vec{v}) = 1.$$

Using (28) the collision rate for hard sphere molecules, when the test particle has velocity $\vec{v}$, is

$$\sigma(\vec{v}) = \pi r^2 \rho_{est} \frac{\sum_{i=1}^{N} w_i |\vec{v} - \vec{v}_i|}{\sum_{i=1}^{N} w_i} \tag{29}$$

Far away from the body (free stream conditions) we can write (23) as

$$r^2 = \frac{1}{\lambda \sqrt{2} \pi \rho_o},$$

where λ is the free stream mean free path, and (2) can then be written

$$\sigma(\vec{v}) = \frac{\rho_{est}}{\rho_o} \cdot \frac{1}{\lambda\sqrt{2}} \cdot \frac{\sum_{i=1}^{N} w_i |\vec{v} - \vec{v}_i|}{\sum_{i=1}^{N} w_i} \tag{30}$$

This is the collision rate for hard-sphere molecules. If K_n is the free stream Knudsen number and d is the body diameter, then

$$\lambda = K_n d$$

and all that is lacking is a means for estimating the ratio of the local density to the free-stream density. This last point will be taken up later. (See equation (40).)

The collision rate for Maxwellian molecules is independent of all velocities (this is the motivation for the Maxwellian collision model) and is obtained by combining equations (22), (24) and (27):

$$\begin{aligned} \sigma &= \rho_{est}\, \pi W_{o\ max}^2\, (2K)^{1/2}\, \left(\frac{kT}{kT}\right)^{1/2} \\ &= \left(\frac{\rho_{est}}{\rho_o}\right) \cdot \frac{W_{o\ max}^2}{2(0.436)\lambda_{eff}} \quad \sqrt{2kT} \end{aligned} \tag{31}$$

One of the normalizations used in the Monte Carlo calculation is to set the mean thermal speed (the root-mean square deviation from the mean speed) equal to 3/2. This is equivalent to setting

$$kT = 1 \tag{32}$$

and when (32) is substituted into (30), the collision rate (per "incident" molecule) for Maxwellian molecules becomes

$$\sigma = \left(\frac{\rho_{est}}{\rho_o}\right) \frac{W_{o\ max}^2}{(0.436)\lambda_{eff}\sqrt{2}} \qquad (33)$$

It should be remembered that the "mean free path" is not a well-defined quantity for all collision models. It is readily visualized for the hard-sphere models, but for any inverse power law molecule (such as the inverse 5th power "Maxwellian") the definition is quite arbitrary. For the Maxwellian molecule, the effective mean free path, defined in (25) is used exclusively here. With this choice, for a given Knudsen number and with all other parameters identical, the hard sphere and Maxwellian models will have the same heat conduction and viscosity in the limit of continuum flow. One must be very careful not to attach any other significance to the mean free path or to the "Knudsen number" when comparing calculations based on different collision models.

(10) Deciding when the next collision will occur

For any binary collision model, the probability that a given molecule of velocity $\vec{v}$ does not suffer a collision in time interval t is $\exp[-\sigma(\vec{v})t]$ where $\sigma(\vec{v})$ is the local collision rate, assumed constant over the small distance $\vec{v}t$. The probability density function for the next collision occurring at t_c is then

$$p(t_c) = \sigma \exp(-\sigma t_c). \qquad (34)$$

We now (with some foresight) make the transformation

$$t_c = -\frac{1}{\sigma} \ln R. \tag{35}$$

The probability density function for R is then easily seen to be

$$q(R) = p(t_c)\left|\frac{dt_c}{dR}\right| = 1. \tag{36}$$

Since the range of t_c is $0 < t_c < \infty$, the range of R must be $0 < R < 1$, and thus R is a "rectangular random number". Thus we can draw a collision time t_c by simply drawing a rectangular random number and using (35).

(11) Choice of a collision partner

If the collision time t_c turns out to be less than the time t_w required to traverse a given cell, then a collision will occur in that cell. It is then necessary to select a collision partner, so that the new velocity of the test molecule may be computed. Given the collision model, the local velocity distribution and the velocity of the incident particle, one can always write the distribution function for the velocity of the collision partner, conditional on the fact that a collision does occur. One then draws a collision partner from this distribution. (This does not in any way alter the distribution function.)

Now the probability of the test particle colliding with a particle of velocity $\vec{v}_i$ (given that a collision occurs) is clearly proportional to the contribution of the velocity $\vec{v}_i$ to the total collision rate. Thus we arrive at a simple rule for selecting a collision partner:

(a) choose a rectangular random number R_n;

(b) choose the velocity $\vec{v}_k$ which satisfies the inequality

$$\sum_{i=1}^{k-1} W_i|\vec{v} - \vec{v}_i| < R_n \sum_{i=1}^{N} w_i|\vec{v} - \vec{v}_i| \leq \sum_{i=1}^{k} w_i|\vec{v} - \vec{v}_i| \qquad (37)$$

for the hard-sphere molecule; or

(c) for the Maxwellian molecule,

$$\sum_{i=1}^{k-1} w_i < R_n \sum_{i=1}^{N} w_i \leq \sum_{i=1}^{k} w_i \ . \qquad (38)$$

By this procedure, the test particle will be scattered in the same way as would a particle in the real gas, provided that the delta function representation of the velocity distribution is an unbiased sample from the true distribution.

(12) Estimation of the distribution function

So far we have calculated the behavior of the test particle, assuming that the distribution function is correctly represented

by a set of weighted delta functions in velocity-space, and that some reasonable estimate of the local number density is available.

We now reverse this view and assume that the test particle's behavior is representative of particles in the actual gas, i.e., that the true distribution function can be deduced by observing the test particle for an infinitely long time.

Now, each cell in the x-y grid can be regarded as a window which occasionally observes the test particle. If on the ith passage through the cell in question the test particle has velocity $\vec{v}_i$ and spends time w_i in traversing the cell, then clearly the best estimate (given no other information) that the cell can make of the velocity distribution is a sum of delta functions at positions $\vec{v}_i$ with areas w_i. This is simply all the cell "sees"; any other representation would involve some prior notion of the form of the distribution function.

The estimation of the ratio of local number density to free-stream number density (hereafter called normalized density) must also be based on observations of the test particle. For this estimate we take

$$\frac{\rho_{est}}{\rho_o} = \frac{\text{(time test particle has spent in given cell)}}{\text{(time it would have spent in same cell under free stream conditions)}} \qquad (39)$$

The numerator in (39) is just the sum of all w_i. The denominator is not so obvious. One can <u>not</u> use the total test particle time, as this would force the average density over the x-y grid to be the free-stream density, which is obviously incorrect. Instead, we count the number of particles N_{pi} which have entered at the ends (upstream or downstream) and multiply by the expected time that a random upstream particle should spend in the given cell. Letting I_x, I_y be the integer coordinates designating the given cell in the grid, our estimate of the number density is then

$$\frac{\rho_{est}}{\rho_o} = \frac{(\sum_{i=1}^{N} w_i)\, L_x L_y}{N_{pi}\, A(I_x, I_y)} \cdot \frac{U}{L_x} \qquad (40)$$

where U is the stream speed, L_x and L_y are the over-all dimensions of the grid, and $A(I_x,I_y)$ is the area of cell (I_x,I_y).

It was mentioned in Part III that the list of delta functions in a given cell was never allowed to grow beyond some maximum length, (hereafter called I_3). However, $\sum_{i=1}^{N} w_i$ is also accumulated in a register for each cell, so that density is estimated from all the times the test particle has entered the cell (since the last time the register was reset to zero), not just from the current members of the list.

Similarly, the moments of the distribution function which are of special interest, namely the velocity and energy, are accumulated in registers. These are not involved in the calculation of collisions but are printed out whenever a "sample" is taken.

The "normalized velocity array", which is printed in tabular form, is simply

$$\vec{v}(I_x,I_y) = \frac{\sum_{i=1}^{N} w_i \vec{v}_i}{\sum_{i=1}^{N} w_i} \tag{41}$$

where N represents <u>all</u> the particles which have entered the cell (I_x,I_y), not just the number on the current list. The normalized temperature is

$$T(I_x,I_y) = \frac{\sum_{i=1}^{N} |\vec{v}_i|^2 w_i}{\sum_{i=1}^{N} w_i} - |\vec{v}(I_x,I_y)|^2 \tag{42}$$

The normalized stagnation temperature is

$$T_S(I_x,I_y) = \frac{\frac{3}{2}\left|\sum_{i=1}^{N} w_i \vec{v}_i\right|^2}{(U^2 + \frac{3}{2}) \sum_{i=1}^{N} w_i} \tag{43}$$

It is also possible to accumulate other moments, if they should be of interest.

(13) Deletion of entries from the lists of delta functions

Every time the test particle traverses the cell, information is gained about the local distribution function. This is added to the prior information as described in Section (12). When the list of delta functions has reached maximum length I_{max}, an entry must be deleted to make room for each new entry. Each entry spends the same time on the list, regardless of its weighting factor.*

(14) Boundary conditions

When the test particle crosses the symmetry plane $x = 0$, it is reflected specularly, i.e., the signs of y and v_y are changed.

When it crosses the end or side boundaries, it is lost and a new test particle is generated by the method described in Section (15).

When it strikes the body, it is absorbed, and a new particle is emitted at the same point by the procedure described in Section (16).

---

*See the alternative procedure described in the Appendix.

(15) Generation of new test particles

a. generation of position

When a new test particle is to be introduced, its position is chosen at random along the wide or end boundary. A certain fraction β must be introduced along the side boundary to compensate for outward diffusion. Otherwise, even without the body, the density would decrease in going from the upstream end to the downstream end. It is clear that the particles introduced at the sides must compensate only for the free-stream diffusion, not for particles deflected sidewards by the body. The side boundary is not a rigid wall. The only approximation caused by the nearness of the side boundary is the neglect of collisions outside this boundary. In free-molecular flow, the boundary has no effect at all.

The fraction β is calculated as follows:

$$J_s = \text{flow thru side} = \frac{L_x}{(\pi)^{3/2}} \iiint_{v_y<0} d\vec{v}\,|v_y| \exp -[(v_x - U)^2 + v_y^2 + v_z^2] \qquad (44)$$

$$J_e = \text{flow thru ends} = \frac{L_y}{(\pi)^{3/2}} \iiint_{\text{all } \vec{v}} d\vec{v}\,|v_x| \exp -1[(v_x - U)^2 + v_y^2 + v_z^2]$$

Integrating equation (44),

$$J_s = \frac{1}{2\sqrt{\pi}} L_x$$

$$J_e = L_y\{ \frac{1}{\sqrt{\pi}} \exp[-u^2] + u\,\mathrm{erf}(u)\} \tag{45}$$

Thus, the fraction of particles entering at the sides is

$$\beta = \frac{J_s}{J_s + J_e} = \frac{1}{1 + 2\frac{L_y}{L_x} \exp(-u^2) + 2\sqrt{\pi}\frac{L_y}{L_x} u\,\mathrm{erf}(u)} \tag{46}$$

$$\beta \approx \frac{1}{1 + 2\sqrt{\pi}\frac{L_y}{L_x} u} \quad \text{if } u \geq 3.$$

The position of the new test particle is then determined as follows:*

(1) draw R_n;

(2) if $R_n < \beta$, introduce at side, a distance $\frac{R_n}{\beta} L_x$ from the upstream end;

(3) if $R_n > \beta$, introduce at upstream end if velocity is positive, downstream if velocity is negative, at

*This procedure will be replaced by a stratified sampling procedure, designed to reduce the effect of uneven flow of particles across the upstream end.

$$y = \frac{R_n - \beta}{1-\beta} L_y.$$

The new velocity must be drawn from the free stream velocity distribution:

$$f(\vec{v}) = (\frac{1}{\pi})^{3/2} \exp\{-[(v_x - u)^2 + v_y^2 + v_z^2]\}. \qquad (47)$$

To choose a normal random deviate, we use a very efficient method suggested by Kahn:[9]

(1) choose random numbers R_1, R_2;

(2) let $A = -\ln R_1$, $B = -\ln R_2$;

(3) if $(A - 1)^2 > 2B$, go back to 1;

(4) if $(A - 1)^2 \leq 2B$, accept A, which is then a normal deviate, with variance 1.

(5) Choose at random the sign to be affixed to A.

To show that this procedure does indeed yield a normal random variate, we compute the probability density function for A, given that A is accepted. By Bayes' rule,

$$P[A \,|\, (A - 1)^2 \leq 2B] = \frac{P[(A - 1)^2 \leq 2B \,|\, A]P(A)}{P[(A - 1)^2 \leq 2B]} \qquad (48)$$

where $P(C|D)$ denotes the "probability of event C, given event D", and $P(C|D)$ denotes the "probability density function for quantity C, given event D".

The denominator of the right side of (48) need not be evaluated as it is not a function of A, but only a constant which normalizes the density function. From Section (10) and from step (2) above, we recognize that A and B have exponential distributions:

$$P(B) = \exp(-B),\ P(A) = \exp(-A). \tag{49}$$

Finally the remaining factor in (48) is easily evaluated as a function of A:

$$P[(A-1)^2 \le 2B|A] = \int_{\frac{(A-1)^2}{2}}^{\infty} \exp(-B)dB$$

$$= \exp\left[\frac{(A-1)^2}{2}\right] \tag{50}$$

Combining (48), (49) and (50):

$$P[A|(A-1)^2 \le 2B] = C_1 \exp\left[-\frac{(A-1)^2}{2}\right] \exp(-A)$$

$$= C_2 \exp\left(-\frac{A^2}{2}\right) \tag{51}$$

This is the desired normal distribution for A, and C_2 is the usual normalization constant. This method for generating normal variates is 76 percent efficient (i.e., it rejects only 24 percent of the pairs of rectangular random numbers) and is probably the fastest method for most digital computers.

Since we want the variance of each of the three components to be 1/2, we multiply the numbers obtained by Kahn's method by $1/\sqrt{2}$. The stream speed U is then added to the x-component of velocity.

The number of particles introduced at the ends and the sides (N_{pi} and N_{side}, respectively) are recorded by a counter. N_{pi} is used to determine when to print out and when to end the computation. Other counters record the energy and momentum of the newly generated particles.

(16) Interaction of particles with the aerodynamic surface

This section describes the way in which the test particle is re-emitted when it strikes the body. In the present calculation the body is a right circular cylinder, but any body with cylindrical symmetry (i.e., no variation in the z-direction) could be treated by this method. Similarly, other surface interaction models could easily be substituted for the present model.

In the present calculation, a fraction of the particles striking the surface are reflected specularly (i.e., the component of velocity normal to the surface is reversed), and the

rest are replaced by new particles emitted diffusely at a temperature such that the thermal speed is S_b times the free stream thermal speed.

One may conceptually visualize a small hole in the surface at the impact point, behind which is a gas in equilibrium with thermal speed S_b. A stream of particles diffuses outward from this hole. We then select at random one of these particles to be the new test particle. Clearly the probability density governing this selection must be proportional to the flux of particles of a given velocity through the hole. This flux is proportional to the velocity distribution times the velocity component normal to the hole.

Let the normal and the two tangential components of velocity be v_n, v_{t1}, v_{t2}, respectively. The density function for particles passing through the hole is then

$$P(v_n, v_{t1}, v_{t2}) = A_1 v_n \exp\left\{\frac{-1}{S_b^2}\left[v_n^2 + v_{y1}^2 + v_{t2}^2\right]\right\} \qquad (52)$$

where A_1 is the normalization constant, and $v_n > 0$.

The normal component is then selected according to the following procedure:

$$P(v_n) = A_2 \exp\left[\frac{-v_n^2}{Sb^2}\right] .$$

Let $u = \frac{v_n^2}{S_b^2}$.

Then the probability density function for u is

$$q(u) = P\left[v_n(u)\frac{dv_n}{du}\right]$$

$$= A_3 \exp(-u).$$

But we have already seen in Section (10) how to draw from this distribution, given a rectangular random number R_1. We simply take

$$u = -\ln R_1$$

and the normal component of velocity then becomes

$$v_n = S_b\sqrt{-\ln R_1} \qquad (53)$$

The two tangential velocity components v_{t1} and v_{t2} could be chosen by the method of Section (15). However, it is more convenient to choose the magnitude of the tangential velocity vector,

$$v_t = \sqrt{v_{t1}^2 + v_{t2}^2} ,$$

and then, recognizing that all angles in the tangential plane are equally likely, choose a random angle between 0 and 2π. Expressed in these polar coordinates, the probability density for v_t is then

$$P(v_t) = A_4 v_t \exp\left[-\frac{v_t^2}{S_b^2}\right] \tag{54}$$

i.e., v_t and v_n have the same density functions. Thus we derive $\vec{v}_t$ from two rectangular random numbers:

$$v_t = S_b\sqrt{-\ln R_2}$$

$$\phi = 2\pi R_3. \tag{55}$$

where it is convenient to measure from a line parallel to the cylinder axis. The new velocity components in x-y-z coordinates are then obtained by a straightforward transformation.

(17) Sampling

After a pre-assigned number Z_{pisam} of test particles has been generated at the end boundaries, a sample is taken.

The current values of the arrays described in Section (12) equations (39) - (43) are printed in such a way that the flow field may be visualized. The contents of the various counters are also printed.

Various aerodynamic coefficients are also calculated and printed out:

The drag coefficient C_D is the total momentum per cross-section area transferred to the cylinder, divided by the total momentum per unit area which has entered upstream since the previous sampling. A factor 2 is added to conform to the convention that $C_D = 2$ if all the stream momentum over the cross section of the body is absorbed by the body.

The energy spread of the entering particles is calculated, mainly as a check on the generating process.

The average free path for all test molecules since the previous sampling is also calculated. This may be expected to be somewhat lower than the free-stream mean free path, due to increased density in front of the body.

The energy transfer to the cylinder, normalized by the energy that would be absorbed under free stream conditions if all particles within the cross section of the cylinder were absorbed.

Finally the three components of force, per entering particle, exerted on the cylinder are calculated, mainly as a check on statistical fluctuations.

After the sampling is completed, the calculation may be continued at the same or at a lower Knudsen number, until the number of particles entering upstream Z_{pi} exceeds the next

pre-assigned number Z_{pigam}. However, if this process were continued, the quantities which have been accumulated in each cell would soon become insensitive to changes in Knudsen number, since the amount of information derived from a single passage of the test particle would become very small in comparison with the information already stored in the cell. To remedy this situation, the following procedure is followed immediately after completing a sampling:

(1) One "pretends" that the latest sample (which was actually based on Z_{pisam} entering particles) was based on only Z_{pieff} particles, where $Z_{pieff} < Z_{pisam}$. (Both these numbers are from lists supplied on data cards.)

(2) Then Z_{pi} and all the current accumulated values in the array of cells are multiplied by Z_{pieff}/Z_{pisam}.

(3) The new (lower) Z_{pi} is now considered to be the number of particles upon which all present estimates are based.

(4) The calculation then proceeds in the normal way.

Note that by this procedure we can attach any desired weight to information gained prior to the latest sample. The lists of individual delta-functions ("particles") in each cell are not affected by this procedure.

V. CONCLUSIONS

Most of the main features of this simulation have been described in Part IV. Results are not yet available; they will be presented in subsequent reports. It is also probable that other features will be added to the program to make the model gas more realistic and to consider other bodies with cylindrical symmetry, such as a flat plate. It is also planned to perform a similar simulation for problems with axial symmetry, such as a sphere or a cone. All such refinements will be described in subsequent reports.

REFERENCES

1. B. J. Alder and T. Wainwright, "Molecular Dynamics by Electronic Computers", Proc. of the Intern. Symposium on Transport Processes in Statistical Mechanics (1956).

2. G. A. Bird, Phys. Fluids 6, 1518 (1963).

3. A. W. Starr (forthcoming Lincoln Laboratory memo).

4. M. Lavin, M.I.T. Fluid Dynamics Research Laboratory Report No. 61-3 (May, 1961).

5. J. K. Haviland, M.I.T. Fluid Dynamics Research Laboratory Report No. 61-5 (May, 1961).

6. J. K. Haviland, Rarefied Gas Dynamics 1, 274 (1963).

7. G. A. Bird, AIAA Journal, 55 (1966).

8. G. N. Patterson, "A State-of-the-Art Survey of Some Aspects of the Mechanics of Rarefied Gases and Plasmas", UTIAS Review No. 18, University of Toronto (March, 1964).

9. H. Kahn, "Applications of Monte Carlo", Research Memorandum, RAND Corporation, 1956.

APPENDIX

An Alternate Representation of the Velocity Distribution

In the model described above, the velocity distribution was represented in each cell by a fixed number of weighted delta functions:

$$f(\vec{v}) = A \sum_{i=1}^{I_{max}} w_i \, \delta(\vec{v} - \vec{v}_i) \qquad \text{(A-1)}$$

The weighting factors w_i were necessary to take proper account that different entries $\vec{v}_i$ represent different intervals of time during which the test particle was observed. By making w_i proportional to the time the test particle spent in the cell during the associated passage, the contribution of each v_i to the current estimate is properly accounted for. Each entry $\vec{v}_i$ remains on the list for I_{max} passages of the test particle, after which it is deleted to make room for a new entry. We shall refer to this scheme as Version I in the following discussion.

An alternate representation of the velocity distribution is to let all the w_i in A-1 be unity, so that all the delta functions have equal area. If this is done, the length of time (number of passages of the test particle) an entry stays on the list must be proportional to the time the test particle took to traverse the cell. We refer to this method as Version II.

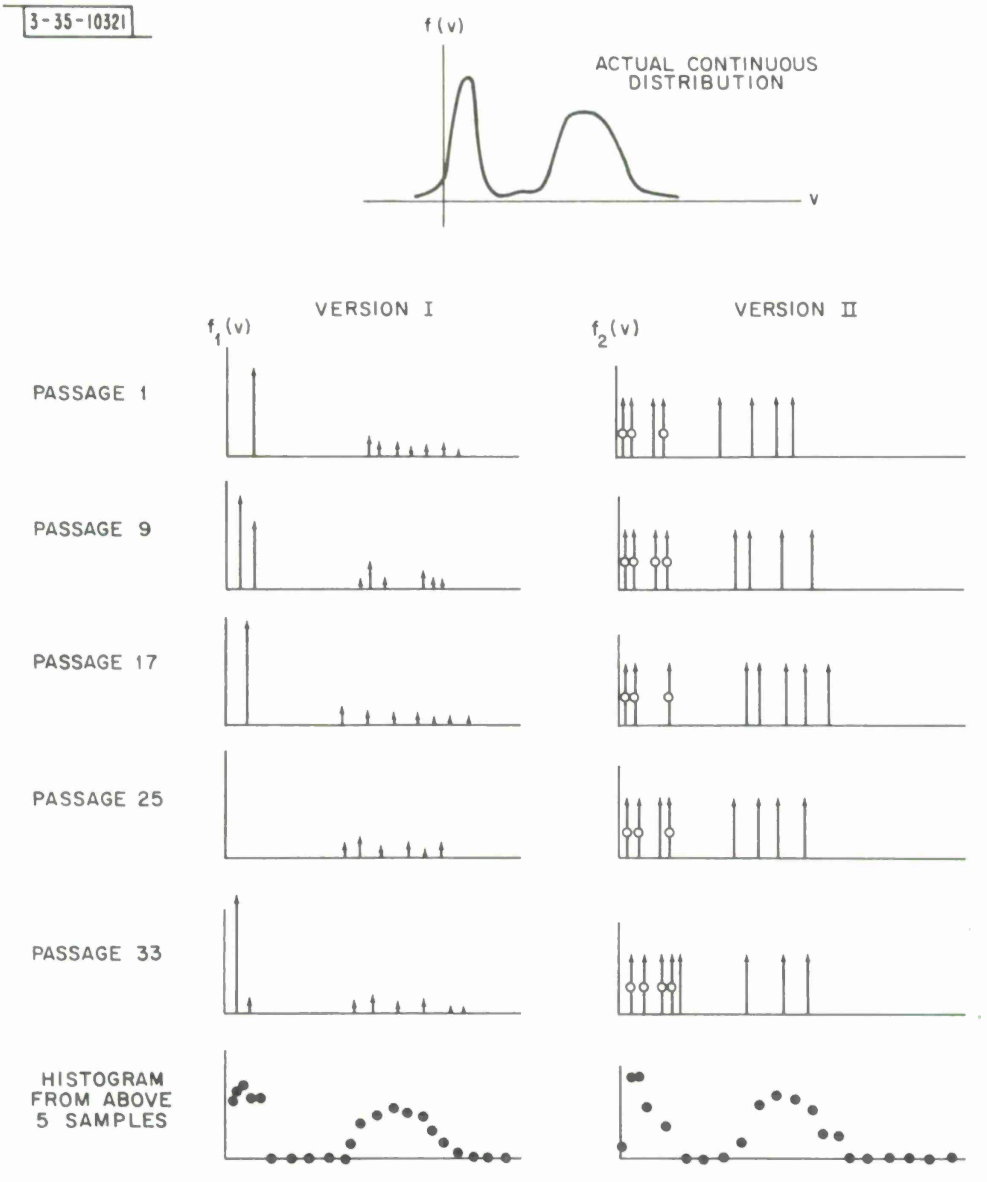

Figure 5. Schematic comparison of two representations of the velocity distribution. (The histograms were not actually calculated.) The small circles indicate spikes which were also present at the last sampling.

It is clear that in both versions, the contribution made by entry $\vec{v}_i$ to the "total representation" is proportional to the weighting factor w_i times the length of time the entry v_i is on the list. (By "total representation" we mean the approximation to the true velocity distribution obtained by averaging the lists over a long time interval.) Thus, in the long run, both versions are statistically correct representations of $f(\vec{v})$. However, at a given instant, the lists in the two versions will have rather different appearances. To illustrate this difference, Figure 5 shows a hypothetical one-dimensional velocity distribution with two peaks, and possible appearances of the lists (consisting of eight entries) at successive passages of the test particle are shown for the two versions. The "histograms" would be calculated by dividing the v-axis into small intervals and taking the average of all spikes which fall within an interval. Note that in <u>both</u> versions the high velocity peak is represented in better detail than the low velocity peak. This is simply because most of the oncoming particles belong to the high-velocity peak, so more information is obtained in a given time about that part of the distribution.

It would appear at a given instant that Version II better represents the slow particles (i.e., treats all particles equally) while Version I favors fast particles, giving a very crude representation of the low-velocity peak. While this is true, it is misleading. In Version II, the "slow" entries must

stay on the list a long time (compared to the fast ones) so the collection of spikes (usually about four) representing the slow particles is not changed often. In Version I, the instantaneous representation of the low velocity peak is very crude (about one spike on the average) but the entire membership of the list is changed after eight passages of the test particle. Thus, after four complete changes of the list (32 passages) the low-velocity peak has been equally well represented in the two versions. Thus it is difficult to choose between the models, and the choice must depend on the details of the computation. It is planned to try both versions. Version II may possibly be preferable because of its better instantaneous representation of the low velocity part of the distribution.

DISTRIBUTION LIST

Advanced Research Projects Agency
Lynn Building
1111 19th Street N.
Arlington, Virginia 22209

Attn: P. J. Friel
A. Gold
D. Mann

Bell Telephone Laboratories, Inc.
Whippany Road
Whippany, New Jersey

Attn: J. P. Penhune

Division 3

S. H. Dodd
M. A. Herlin

Group 35

M. Balser
S. Edelberg
G. F. Pippert
R. E. Slattery
R. S. Cooper
J. Herrmann
K. Kresa
L. R. Martin
C. W. Rook (3)
S. C. Wang
A. Starr (10)

DOCUMENT CONTROL DATA – R&D

(Security classification of title, body of abstract and indexing annotation must be entered when the overall report is classified)

1. ORIGINATING ACTIVITY *(Corporate author)*
Lincoln Laboratory, M.I.T.

2a. REPORT SECURITY CLASSIFICATION
Unclassified

2b. GROUP
None

3. REPORT TITLE
Monte Carlo Simulation of the Flow of a Rarefied Gas Around a Cylinder

4. DESCRIPTIVE NOTES *(Type of report and inclusive dates)*
Technical Note

5. AUTHOR(S) *(Last name, first name, initial)*
Starr, Alan W.

6. REPORT DATE	7a. TOTAL NO. OF PAGES	7b. NO. OF REFS
18 January 1967	64	9

8a. CONTRACT OR GRANT NO.
AF 19(628)-5167

b. PROJECT NO.
ARPA Order 600

c.

d.

9a. ORIGINATOR'S REPORT NUMBER(S)
Technical Note 1967-7

9b. OTHER REPORT NO(S) *(Any other numbers that may be assigned this report)*
ESD-TR-67-41

10. AVAILABILITY/LIMITATION NOTICES
Distribution of this document is unlimited.

11. SUPPLEMENTARY NOTES
None

12. SPONSORING MILITARY ACTIVITY
Advanced Research Projects Agency, Department of Defense

13. ABSTRACT

A Monte Carlo technique is described for simulating the high-speed flow of a rarefied gas around a cylindrical body. The method uses a hard-sphere model, or alternatively, the "Maxwellian" model to compute collisions between particles. A representative "test particle" is scattered in such a way that its statistical behavior approximates that of a random particle chosen from the actual gas. This requires knowledge of the distribution function of "target" particles, which is estimated from observations of the behavior of the test particle.

The method is applicable to any collision model and to any model for the interaction between the gas and the surface of the body.

14. KEY WORDS

gas dynamics
gas flow
gas simulation
Monte Carlo technique